Can current climate model forcings explain the spatial and temporal signatures of decadal OLR variations?

Richard P. Allan and A. Slingo

Hadley Centre, Met Office, Bracknell, Berkshire, U.K.

Received 21 December 2001; revised 18 February 2002; accepted 5 March 2002; published 12 April 2002.

[1] Top of atmosphere broadband radiative fluxes derived from satellite measurements exhibit surprisingly large decadal variability in the tropics which appears to be related to changes in cloudiness. Climate models fail to reproduce these changes, even when all of the currently known climate forcing agents are prescribed. The interannual variability and spatial signal of the observed changes are analysed and compared to various configurations of the Hadley Centre climate model. Applying EOF analysis to the spatial patterns of the variability shows that these are dominated by El Niño in both the satellite data and the model. However, the second EOF reveals the pattern due to the observed decadal-scale variation in outgoing longwave radiation (OLR), but this is not captured by the climate model. This suggests that either the model lacks some internal physical process or some additional external forcing that is responsible for the observed changes in OLR. *INDEX TERMS:* 1610 Global Change: Atmosphere (0315, 0325); 3359 Meteorology and Atmospheric Dynamics: Radiative processes; 3360 Meteorology and Atmospheric Dynamics: Remote sensing

[2] Large decadal-scale variations in the tropical radiation budget, consistent with changes in cloud amount, are not simulated by several "state of the art" climate models [*Wielicki et al.*, 2002]. Assuming this result to be robust, it is important to establish whether this discrepancy is the result of forcings not included in the models or whether the models neglect the required physics necessary to accurately simulate decadal-scale fluctuations in the Earth's radiation budget. The present study assesses whether the natural and anthropogenic forcings currently applied to versions of the Hadley Centre climate model are able to explain the spatio-temporal signal of these changes. We analyse the observed and simulated top of atmosphere outgoing longwave radiation (OLR), clear-sky OLR and reflected shortwave radiation (RSW) variability, concentrating on the period 1985–1998. While we do not consider all the data used in *Wielicki et al.* [2002], this period allows us to use the complete and homogenous record from the non-scanner Wide Field Of View (WFOV) instrument, validated by scanner measurements throughout the period, in an EOF analysis. The period also contains large variability in the tropical radiation budget due to volcanos, El Niño and the unexplained decadal variability.

1. Interannual Variability

[3] Figure 1 shows the low-latitude mean (40°S to 40°N) radiative flux variability for the scanner data from the Earth Radiation Budget Satellite (ERBS), the Scanner for Radiation Budget (ScaRaB) instrument, the Clouds and the Earth's Radiant Energy System (CERES) scanning instrument and the WFOV non-scanner instrument on the ERBS satellite. Integrations of the Hadley Centre coupled atmosphere-ocean climate model (HadCM3) and atmosphere-only climate model (HadAM3) forced by the GISST 3.1 sea surface temperature (SST)/sea-ice dataset [see *Sexton et al.*, 2001] and combinations of natural and anthropogenic scenarios are displayed. Interannual anomalies were calculated for each product with reference to a monthly climatology. All climate model simulations were initiated in 1860, including changes in the forcings applied from that time, but subsets of the entire records are used in the following analysis. Details of the reference climatologies, satellite data and model integrations are provided in Table 1. In Figure 1, variability from a 100-year section of the HadCM3 control run (CTR) and the 1985–1999 section of the greenhouse gas forced run (GHG, 4 ensemble members) are represented as one standard deviation error bars. The GISST integration of HadAM3, forced by SST/sea ice only, is shown by the shaded region which denotes the inter-ensemble (5 member) standard error. The four ensemble members of HadAM3 forced by natural and anthropogenic forcings (SST/sea ice, volcanic, solar, greenhouse gas, tropospheric and stratospheric ozone, direct and indirect aerosol; GISST+) are displayed as dotted lines.

[4] The inability of the climate models to reproduce the 20°S to 20°N radiation budget variability [*Wielicki et al.*, 2002] also applies to the larger spatial-scale considered in Figure 1. Further, such variability is not simulated by HadCM3 unforced variability (CTR) or the GHG scenario. The discrepancy conspicuous in Figure 1 could be reduced by "correcting" the observations assuming constant calibration error after 1992. However, *Wielicki et al.* [2002] argue that such an error is highly unlikely and we shall assume the observations to be correct. For the physical parametrizations employed in HadAM3 and considering all possible combinations of the forcings currently applied in GISST+, the observed radiation budget changes cannot be explained.

[5] Superimposed on this decadal-scale change in OLR and RSW are variations due to the El Niño Southern Oscillation (ENSO), in particular a strong peak in OLR during 1998, and reduced OLR and increased RSW following the 1991 eruption of Mt. Pinatubo [*Minnis et al.*, 1993]. HadAM3 captures the peak in clear-sky OLR observed by CERES during the 1998 El Niño and the GISST+ integration simulates the increase in RSW during 1991, albeit imperfectly. Figure 1a and 1b highlight the strong dependence of simulated OLR variability on the clear-sky component, which is primarily determined by the tropic-wide temperature due to minimal variation in the model relative humidity. Conversely, the observed OLR variability greatly exceeds that of the clear-sky component. Thus, the model cannot reproduce the observed variation in cloud radiative effect. Unfortunately, independent confirmation of the changes in cloud parameters is not yet available.

2. Spatial Variability

[6] Maps of 60°S to 60°N OLR changes (1992–1997 minus 1985–1990) are displayed in Figure 2 for WFOV, the polar orbiting NOAA satellites and HadAM3. NOAA OLR is an updated estimate from narrow-band (10 μm) radiances [*Lucas et al.*, 2001]. For NOAA and HadAM3, positive differences are shaded; positive differences more than 3 Wm^{-2} are shaded for WFOV. Note that Figure 2a shows positive values almost everywhere, consistent

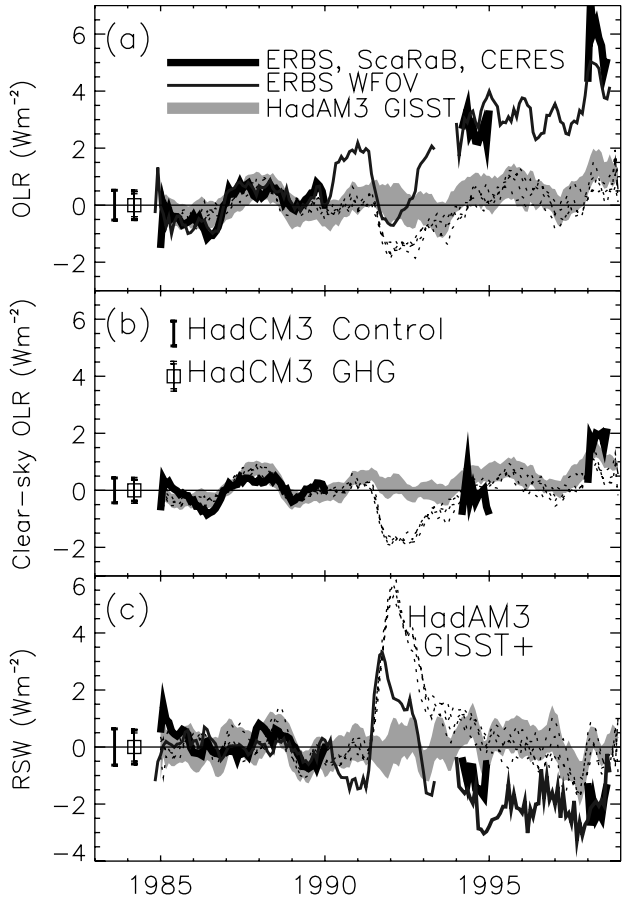

Figure 1. Time series of the 40°S–40°N top-of-atmosphere interannual flux variability (Wm^{-2}) for (a) OLR, (b) clear-sky OLR and (c) RSW from the sources described in Table 1. For further details, see text.

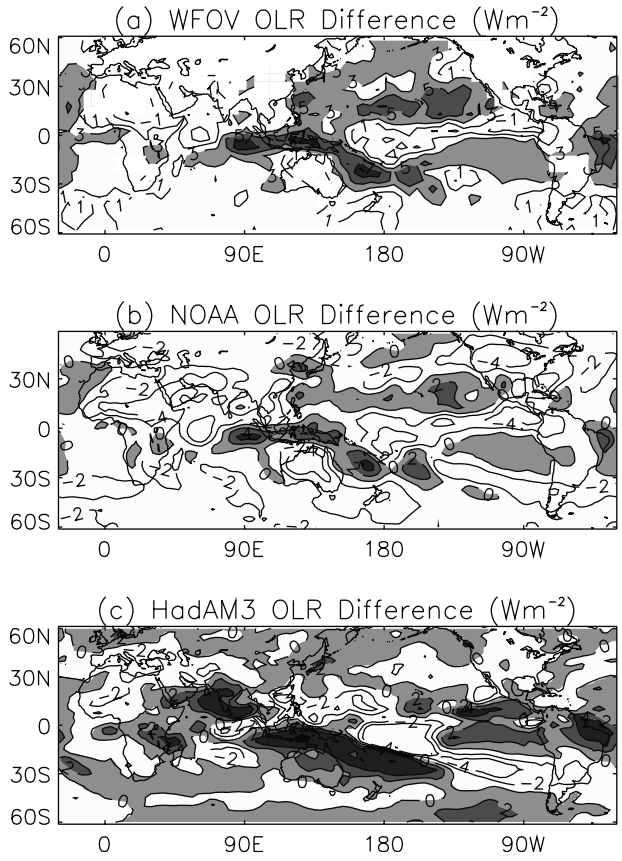

Figure 2. Change in OLR (Wm^{-2}) for (a) WFOV, (b) NOAA and (c) HadAM3 GISST ensemble mean for the period 1992–1997 minus 1985–1990. Contour interval, 2 Wm^{-2}; for further details, see text.

with Figure 1a. The significant mean OLR increase for WFOV (+2.4 Wm^{-2}) is not apparent for NOAA (−1.2 Wm^{-2}) although incomplete diurnal sampling and other limitations make these NOAA data unreliable for studying trends [*Wielicki et al.*, 2002]. The NOAA data are included here because they have been used extensively in studies of regional anomalies of the tropical circulation and heating [e.g. *Matthews and Kiladis*, 1999]. Also, the remarkable similarity of the spatial anomaly patterns for WFOV and NOAA increases confidence in the ability of both datasets to represent the regional OLR anomalies.

[7] The anomaly pattern is strongly dependent on the phase and strength of ENSO for each period. The positive OLR anomalies over the west Pacific and negative anomalies over the east Pacific are suggestive of stronger El Niño conditions in the later period, consistent with the extended 1992–1994 event and strong 1997/8 event [*Wang and Weisberg*, 2000]. HadAM3 also crudely exhibits such a dipole although it is exaggerated over the southern Pacific. However, the mean increases in WFOV OLR are not reproduced by HadAM3 for any combination of the forcings considered: ranges for the GISST and GISST+ ensemble members are +0.2 to +0.4 Wm^{-2} and −0.1 to +0.1 Wm^{-2} respectively.

3. EOF Analysis

[8] Employing Empirical Orthogonal Function (EOF) analysis, the dominating ENSO signal may be removed statistically. Using

Table 1. Details of the Satellite Observations and Model Simulations Employed in Figure 1

Data	Details	Period	Reference Data	Source
ERBS	Scanning radiometer	1985–1989	ERBS 1985–1989	1
WFOV	Non-scanning radiometer	1985–1998	WFOV 1985–1989	1
ScaRaB	Scanning radiometer	1994–1995	ERBS 1985–1989	2
CERES	Scanning radiometer	1998	ERBS 1985–1989	3
HadAM3 (GISST)	Atmospheric climate model forced by SST/sea ice	1985–1998	GISST 1985–1989	4,5
HadAM3 (GISST +)	As GISST, plus natural and anthropogenic forcing	1985–1998	GISST+ 1985–1989	4,5,6
HadCM3 (CTR)	Coupled climate model: Control	1900–2000	CTR 1900–2000	6
HadCM3 (GHG)	CTR + Greenhouse gas forcing	1985–1999	GHG 1985–1989	6

Source: 1, *Barkstrom et al.* [1990]; 2, *Kandel et al.* [1998]; 3, *Wielicki et al.* [1996]; 4, *Pope et al.* [2000]; 5, *Sexton et al.* [2001]; 6, *Johns et al.* [2001].

annual means of OLR over the ocean from WFOV, the first and second EOF patterns and their time-series are computed (Figure 3). The first EOF is an ENSO pattern with positive values over the tropical west Pacific extending to the sub-tropical Pacific around negative anomalies over the central Pacific. This is confirmed by the time-series in Figure 3c which shows the pattern to be strongly positive for El Niño events. The NOAA data reproduce a similar EOF1 pattern and time-series (not shown). The WFOV OLR variance explained is 45% for EOF1 and 17% for EOF2. EOF2 values are predominantly of the same sign, and strongest in the sub-tropics. The EOF2 time-series in Figure 3c shows an increase in values after 1992 and is reminiscent of the increase in OLR displayed in Figure 1a. Thus the observed increase in OLR anomalies appears to be manifest on a quasi tropic-wide scale. This is a surprising result, given the assertion that changes in cloud cover explain the decadal variations in OLR. While cloudiness varies markedly over the geographical region considered, there is no obvious spatial signature of this in the decadal-scale component of the observed variability. This merits further study.

[9] The first two EOF patterns and their time-series for the HadAM3 GISST ensemble mean are displayed in Figure 4 and are generally representative of all ensemble members. The first EOF resembles the El Niño pattern shown by the WFOV data in Figure 3a although the model produces a stronger signal over the South Pacific. EOF2 for the HadAM3 ensemble mean appears to be a modified ENSO pattern shifted to the east and shows no similarity to the corresponding WFOV time-series. Further, when combinations of natural and anthropogenic forcings are applied, there remains no similarity between WFOV and HadAM3 EOF2 patterns. The EOF2 pattern for the NOAA data (not shown) also shows no similarity to the WFOV EOF2.

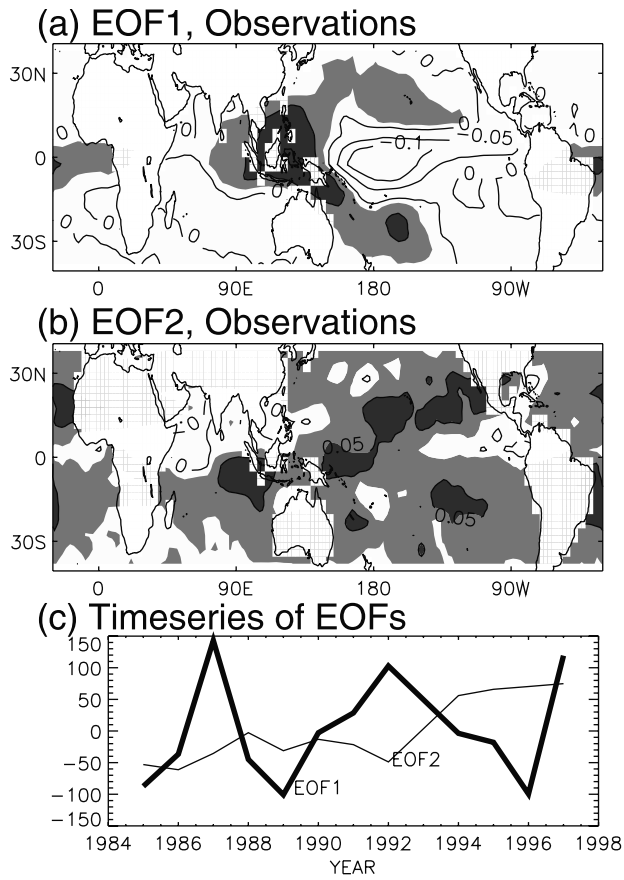

Figure 3. First and second EOFs and their time-series for annual-mean outgoing longwave radiation from WFOV. EOF values greater than 0.02 are lightly shaded and values greater than 0.05 are darkly shaded.

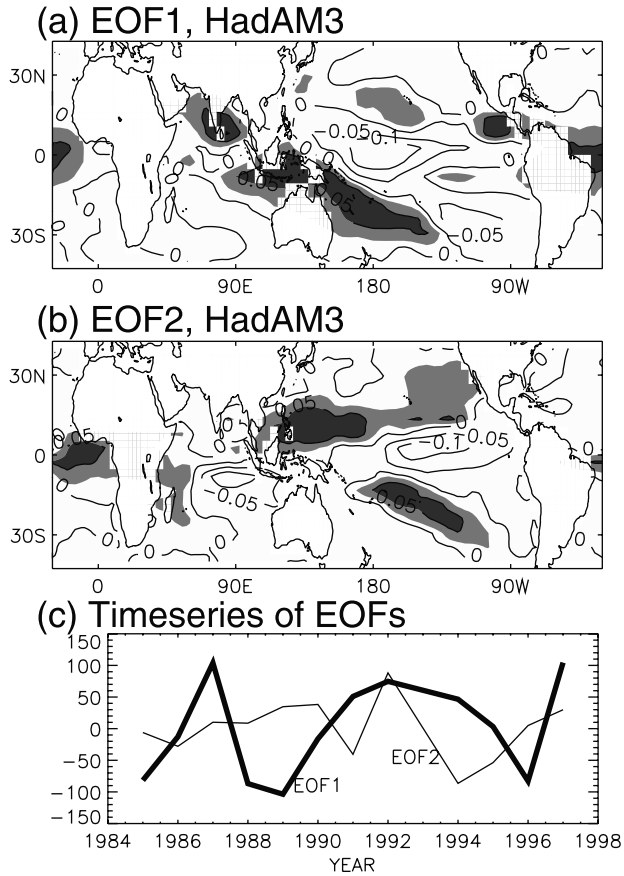

Figure 4. As Figure 3 but for GISST ensemble mean.

4. Discussion

[10] Climate models forced with observed SSTs are unable to reproduce the 1979–2000 tropical radiation budget variability measured by satellites which appear to be dominated by changes in cloud radiative effects [*Wielicki et al.*, 2002]. We extend this conclusion by showing that the observed low-latitude variability is not captured by the Hadley Centre climate model when employing a variety of natural and anthropogenic forcings in addition to SST. Further, the magnitude of observed variability is not present in a 100 year control run of the coupled ocean-atmosphere version of the same model. The HadAM3 integrations cannot reproduce the decadal-scale pattern of OLR changes diagnosed using EOF analysis. Assuming the observations to be robust, this suggests that the forcings currently used are inadequate, or an additional forcing not represented by those prescribed in the present analysis is required to explain the tropical flux variability, or that there are important physical processes that are not accounted for in the climate model. To determine which model deficiency is responsible for the discrepancy, further work is required to ascertain the sensitivity of the more uncertain forcings used in the present study and to explore additional forcings which are not considered.

[11] The decadal-scale changes in the tropical radiation budget also coincide with a sub-tropical drying [*Bates and Jackson*, 2001], a possible strengthening of the tropical circulation [*Chen et al.*, 2002] and perhaps are also related to changes in the temperature lapse-rate which are not captured by climate models [*Gaffen et al.*, 2000] [see discussion in *Wielicki et al.*, 2002]. Reductions in tropical upper level cloudiness and increases in OLR have been

hypothesized by *Lindzen et al.* [2001] as capable of providing a negative feedback on the warming induced by increased greenhouse gases. However, it seems unlikely that this mechanism can explain the observed changes in tropical OLR, since these are much larger than the change in the greenhouse gas forcing over this period. In addition, *Lin et al.* [2002] showed that CERES data did not support the *Lindzen et al.* [2001] hypothesis.

[12] The representation of radiative feedbacks within the climate system constitutes a considerable source of uncertainty in the prediction of the climatic response to radiative forcing [*IPCC*, 2001]. Accurate and continuous monitoring of the Earth's radiation budget provides one method of addressing this uncertainty by comparing the simulated and observed changes in the radiation budget. Further work is needed to confirm the robust nature of the observed changes and to determine whether they are externally forced or due to a mode of natural climate variability not represented by models.

[13] **Acknowledgments.** Thanks to Bruce Wielicki, Mark Webb and William Ingram for stimulating discussion and to David Sexton for providing the GISST integrations. The ERBS, WFOV and CERES data were retrieved from the NASA Langley DAAC. The ScaRaB data is courtesy of the Centre Spatial De Toulouse and the NOAA data was provided by Duane Waliser. The work was supported by the UK Department for Environment, Food and Rural Affairs contract PECD 7/12/37.

References

Barkstrom, B. R., E. F. Harrison, R. B. Lee, and the ERBE Science Team, Earth Radiation Budget Experiment (ERBE) archival and April 1985 Results, *Bull. Am. Meteorol. Soc.*, *70*, 1254–1262, 1990.

Bates, J. J., and D. L. Jackson, Trends in upper tropospheric humidity, *Geophys. Res. Lett.*, *28*, 1695–1698, 2001.

Chen, J., B. E. Carlson, and A. D. Del Genio, Evidence for strengthening of the tropical general circulation in the 1990s, *Science, 295*, 838–841, 2002.

Gaffen, D. J., B. D. Santer, J. S. Boyle, J. R. Christy, N. E. Graham, and R. J. Ross, Multidecadal changes in the vertical temperature structure of the tropical troposphere, *Science*, *287*, 1242–1245, 2000.

IPCC, J. T. Houghton, Y. Ding, D. J. Griggs, M. Noguer, P. J. van der Linden, X. Dai, K. Maskell, and C. A. Johnson (Eds.), *Climate change 2001: The Scientific Basis*, 881 pp., Cambridge University Press, Cambridge, 2001.

Johns, T. C., J. M. Gregory, W. J. Ingram, C. E. Johnson, A. Jones, J. A. Lowe, J. F. B. Mitchell, D. L. Roberts, D. M. H. Sexton, D. S. Stevenson, S. F. B. Tett, and M. J. Woodage, Anthropogenic climate change for 1860 to 2100 simulated with the HadCM3 model under updated emissions scenarios, *HCTN 22*, 61 pp., Hadley Centre, Met Office, Bracknell, U.K., 2001.

Kandel, R., M. Viollier, P. Raberanto, J. Ph. Duvel, L. A. Pakhomov, V. A. Golovko, A. P. Trishchenko, J. Mueller, E. Raschke, R. Stuhlmann, and the International ScaRab Scientific Working Group (ISSWG), The ScaRaB radiation budget dataset, *Bull. Am. Meteorol. Soc.*, *79*, 765–783, 1998.

Lin, B., B. A. Wielicki, L. H. Chambers, Y. Hu, and K.-M. Xu, The Iris hypothesis: a negative or positive cloud feedback?, *J. Climate*, *15*, 3–7, 2002.

Lindzen, R., M.-D. Chou, and A. Hou, Does the earth have an adaptive infrared iris?, *Bull. Am. Meteorol. Soc.*, *82*, 417–432, 2001.

Lucas, L. E., D. E. Waliser, P. Xie, J. E. Janowiak, and B. Liebmann, Estimating the satellite equatorial crossing time biases in the daily, lobal outgoing longwave radiation dataset, *J. Climate*, *14*, 2583–2605, 2001.

Matthews, A. J., and G. N. Kiladis, Interactions between ENSO, transient circulation, and tropical convection over the Pacific, *J. Climate*, *12*, 3062–3086, 1999.

Minnis, P., E. F. Harrison, G. G. Gibson, F. M. Denn, D. R. Doelling, and W. L. Smith Jr., Radiative forcing by the erruption of Mt. Pinatubo, *Science*, *259*, 1411–1415, 1993.

Pope, V. D., M. L. Gallani, P. R. Rowntree, and R. A. Stratton, The impact of new physical parametrizations in the Hadley Centre Climate Model - HadAM3, *Climate Dynamics*, *16*, 123–146, 2000.

Sexton, D. M. H., D. P. Rowell, C. K. Folland, and D. J. Karoly, Detection of anthropogenic climate change using an atmospheric GCM, *Climate Dynamics*, *17*, 669–685, 2001.

Wang, C., and R. H. Weisberg, The 1997–98 El Niño evolution relative to previous El Niño Events, *J. Climate*, *13*, 488–501, 2000.

Wielicki, B. A., B. R. Barkstrom, E. F. Harrison, R. B. Lee, G. L. Smith, and J. E. Cooper, Clouds and the Earth's Radiant Energy System (CERES): an Earth observing system experiment, *Bull. Am Meteorol. Soc.*, *5*, 853–868, 1996.

Wielicki, B. A., T. M. Wong, R. P. Allan, A. Slingo, J. T. Kiehl, B. J. Soden, C. T. Gordon, A. J. Miller, S.-K. Yang, D. A. Randall, F. Robertson, J. Susskind, and H. Jacobowitz, Evidence for large decadal variability in the tropical mean radiative energy budget, *Science*, *295*, 841–844, 2002.

R. P. Allan and A. Slingo, Hadley Centre, Met Office, London Road, Bracknell, Berkshire, RG12 2SY, U.K. (richard.allan@metoffice.com)